OPTIMIZATION OF COMPOSITE MATERIAL DE-ICING COMPONENT FOR HELICOPTER ROTOR

Long Chen [1], Yidu Zhang [2] and Qiong Wu [3]

[1] Room 313, Block B, The New Main Building, No. 37 Xueyuan Road, Haidian District, Beijing, China, State Key Laboratory of Virtual Reality Technology, School of Mechanical Engineering and Automation, Beihang University, China, dragonchen@buaa.edu.cn
[2] Room 313, Block B, The New Main Building, No. 37 Xueyuan Road, Haidian District, Beijing, China, State Key Laboratory of Virtual Reality Technology, School of Mechanical Engineering and Automation, Beihang University, China, ydzhang@buaa.edu.cn
[3] Room 313, Block B, The New Main Building, No. 37 Xueyuan Road, Haidian District, Beijing, China, State Key Laboratory of Virtual Reality Technology, School of Mechanical Engineering and Automation, Beihang University, China, wuqiong@buaa.edu.cn

Keywords: Composite material de-icing component, Temperature field optimization, Finite element numerical simulation, Orthogonal experiment

ABSTRACT

An optimization for helicopter rotor composite material de-icing component based on numerical simulation was proposed. Due to the influence of external flow filed and wire pattern in the de-icing component, uneven distribution of the temperature field on the iron surface of the rotor composite material de-icing component becomes the main factor affecting the efficiency of de-icing. The heat transfer numerical simulation model of the rotor composite material de-icing component was established for de-icing structure optimization. The optimization procedure was determined by using orthogonal test method combined with numerical simulation method. The optimized temperature field distribution on the iron surface of the composite material de-icing component meets the de-icing requirements which reaching 2℃ which above zero.

INTRODUCTION

Ice protection system (IPS) is an essential equipment of all transport category aircraft. It is widely used to ensure compliance with airworthiness requirements in icing conditions [1]. Icing causes helicopter rotor lift decrease and instability, which could result in stalling or crash [2-5]. The primary means to preventing accreting ice is installing a composite material de-icing component on the rotor surface. The voltage and electric current of the heating wire are controlled in the composite material de-icing component to achieve anti-icing and deicing effect [6-7]. The material composition of the composite material de-icing component is shown in Fig. 1.

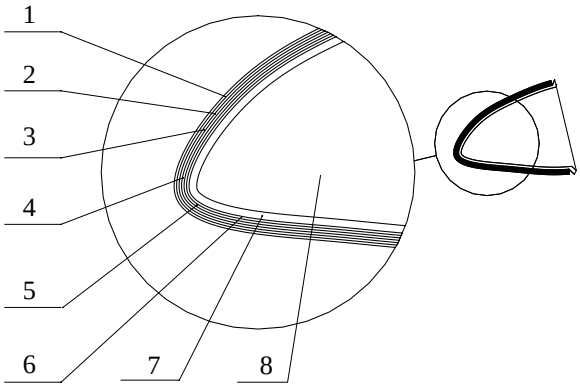

1. Iron steel 2. Chloride butyl rubber 3. Glass fiber 4. Ni-Cr alloy 5. Carbon fiber 6. Chloride butyl rubber 7. Aviation aluminum alloy 8. Aluminum foam
Fig. 1. Materials of de-icing component.

The composite material de-icing component consists of multilayer composite components with multi-materials. The thermal performance of each composite material layer is complex. When the rotor functions in high-speed rotation and in a low-temperature environment, the heat transfer process of the rotor composite material de-icing component is related to the coupling effect of the external convection heat transfer of the flow field and internal heat conduction in the multilayer composite components. Heat transfer analysis of the rotor composite material de-icing component becomes highly complicated because of the effect of electric wire pattern in the rotor composite material de-icing component. Previous studies indicate that the iron surface temperature field distribution of the rotor composite material de-icing significantly affects the efficiency of eliminating ice. The uneven temperature field distribution of the iron surface leads to the failure of ice melting in some local areas on the rotor, and exacerbates the icing of these areas, which seriously threatens flight safety through the loss of maneuverability and controllability of a helicopter [8-10].

In this paper, an optimization for helicopter rotor composite material de-icing component based on numerical simulation was proposed. Due to the influence of external flow filed and wire pattern in the de-icing component, uneven distribution of the temperature field on the iron surface of the rotor composite material de-icing component becomes the main factor affecting the efficiency of de-icing. The heat transfer numerical simulation model of the rotor composite material de-icing component was established for de-icing structure optimization. The optimization procedure was determined by using orthogonal test method combined with numerical simulation method. The optimized temperature field distribution on the iron surface of the composite material de-icing component meets the de-icing requirements which reaching 2 ℃ above zero.

MATHMATIC MODELING

The internal heat transfer of rotor composite material de-icing component directly affects the temperature distribution of de-icing on the rotor surface. Considering the material anisotropy of composite material internal heat transfer and the diversity of main directions of conductivity of material in different layers, a heat transfer analysis model of composites was set up.

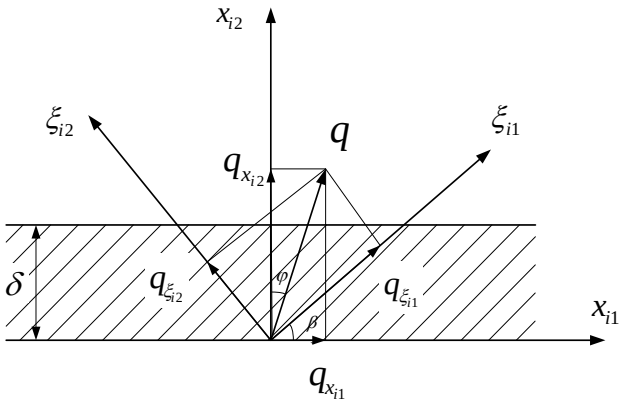

Fig.2. Two-dimensional steady-state heat conduction of anisotropic material.

Set δ stands for the thickness of the *i*th layer of the composite material de-icing component. The ξ_{i1} and ξ_{i2} stand for the main direction of material thermal conductivity (see Fig.2), and the Fourier law as follows:

$$q_{\xi_{i1}} = -\lambda_1 \frac{\partial t}{\partial \xi_{i1}} \tag{1}$$

$$q_{\xi_{i2}} = -\lambda_2 \frac{\partial t}{\partial \xi_{i2}} \tag{2}$$

Thus the heat flux density can be written:

$$q = -\lambda_1 \frac{\partial t}{\partial \xi_{i1}} - \lambda_2 \frac{\partial t}{\partial \xi_{i2}} \tag{3}$$

Through the coordinates change, coordinate system (ξ_{i1}, ξ_{i2}) transforms to coordinate system (x_{i1}, x_{i2}). Due to simplifying as 2D steady heat conduction, we can get the following heat transfer coefficients:

$$q_{x_{i1}} = (\lambda_1 - \lambda_2)\sin\beta\cos\beta\frac{t_1 - t_2}{\delta} \tag{4}$$

$$q_{x_{i2}} = (\lambda_1 \sin^2\beta + \lambda_2 \cos^2\beta)\frac{t_1 - t_2}{\delta} \tag{5}$$

The angle φ between q and temperature gradient direction satisfies:

$$\tan\varphi = \frac{q_{x_{i1}}}{q_{x_{i2}}} = \frac{(\lambda_1 - \lambda_2)\sin\beta\cos\beta}{\lambda_1 \sin^2\beta + \lambda_2 \cos^2\beta} \tag{6}$$

Thus, the coefficient of thermal conductivity of the ith layer of anisotropic composite material is obtained in the coordinate system (x_{i1} , x_{i2}). By the multilayer composite material stable heat conduction theory, the contact surface temperature between the ith layer and the $(i-1)$th layer can be written:

$$T_{wi} = T_{w1} - \phi\sum_{j=1}^{i-1}\frac{\delta_j}{A\lambda_j} = T_{w1} - \phi\sum_{j=1}^{i-1}R_{\lambda j} \tag{7}$$

Substitute Eq. (17) into Eq. (19) and obtain the following equation:

$$T_{wi} = T_{w1} - \phi\sum_{j=1}^{i-1}\frac{\delta_j}{A\lambda_j} = T_{w1} - \phi\sum_{j=1}^{i-1}\frac{\delta_j}{A(\lambda_{j1}\sin^2\beta + \lambda_{j2}\cos^2\beta)} \tag{8}$$

Where T_{w1} is the temperature of heating wire, T_{wi} is the temperature between the ith layer and the $(i-1)$th layer of rotor composite material de-icing component, δ_j is the thickness of the $(i-1)$th layer, A is the contact surface area between the ith layer and the $(i-1)$th layer, λ_j is the heat conductivity coefficient of the $(i-1)$th layer of rotor composite material de-icing component.

RESULTS AND DISCUSSION

The optimization parameters are selected and determined respectively as shown in Table 1, where V denotes flow velocity, T indicates environment temperature, W signifies rotor speed, λdenotes heat conductivity coefficient of heat transfer layer, H indicates the thickness of adhesive layer, U signifies electric voltage, and L denotes the distance of heating wire. By using iron surface temperature difference (ΔT) as the optimization index, orthogonal test analysis is conducted; the results are shown in Table 3.

Table 1. Results of orthogonal design optimization method

Test	V(m/s)	T (℃)	λ(W/(m Ƙ))	U(V)	H (mm)	L (mm)	ΔT (℃)
Test1	15	-8	5.8	50	0.2	10	2.4
Test2	15	-10	7.6	80	0.3	15	3.4.
Test3	15	-12	11.9	100	0.4	20	4.5
Test4	15	-15	12.8	130	0.5	25	5.1
Test5	15	-20	15.2	150	0.6	30	5.3
Test6	20	-8	7.6	130	0.4	30	4.8
Test7	20	-10	11.9	150	0.5	10	4.1
Test8	20	-12	12.8	50	0.6	15	8.9
Test9	20	-15	15.2	80	0.2	20	3.2
Test10	20	-20	5.8	100	0.3	25	6.1
Test11	25	-8	11.9	80	0.6	25	5.4
Test12	25	-10	12.8	100	0.2	30	4.3
Test13	25	-12	15.2	130	0.3	10	4.5
Test14	25	-15	5.8	150	0.4	15	5.6
Test15	25	-20	7.6	50	0.5	20	1.7
Test16	30	-8	12.8	150	0.3	15	8.7
Test17	30	-10	15.2	50	0.4	25	0.7
Test18	30	-12	5.8	80	0.5	30	5.4
Test19	30	-15	7.6	100	0.6	10	1.4
Test20	30	-20	11.9	130	0.2	20	3.5
Test21	35	-8	15.2	100	0.5	15	4.1
Test22	35	-10	5.8	130	0.6	20	6.4
Test23	35	-12	7.6	150	0.2	25	5.9
Test24	35	-15	11.9	50	0.3	30	1.3
Test25	35	-20	12.8	80	0.4	10	4.1
Mean Value1	4.18	5.13	5.22	4.43	3.89	3.35	
Mean Value2	3.84	3.83	3.49	4.34	4.83	4.59	
Mean Value3	4.37	4.25	3.79	4.08	3.96	3.89	
Mean Value4	3.95	3.35	4.65	4.90	4.14	4.63	
Mean Value5	4.39	4.16	3.57	5.97	3.90	4.27	
Range	0.55	1.78	1.73	1.89	0.94	1.28	

Table 2. Analysis results of orthogonal optimization

Factor	V (m/s)	T (℃)	λ(W/(m·K))	H (mm)	U (V)	L (mm)
Factor1	15	-8	5.8	0.2	50	10
Factor2	20	-10	7.6	0.3	80	15
Factor3	25	-12	11.9	0.4	100	20
Factor4	30	-15	12.8	0.5	130	25
Factor5	35	-20	15.2	0.6	150	30

The parameters listed in Table 2 correspond to the mean values in Table 1. The table above shows that nine factors are ranked from large to small: range of electric voltage 1.89 > range of temperature 1.78 > range of heat conductivity coefficient of heat transfer layer 1.73 > range of distance of heating wire 1.28 > range of thickness of adhesive layer 0.94 > range of rotor speed 0.55. Therefore, the most effective factor among the nine factors on the temperature field uniform distribution on the rotor iron surface is electric voltage, followed by ambient temperature. Rotor speed has the least influence among the factors. The optimization parameters are proposed by analyzing the trend of each factor effecting the temperature distribution as shown in Table 3.

Table 3. The optimization parameters

Test	V (m/s)	T (℃)	λ(W/(m·K))	H (mm)	U (V)	L (mm)
Test26	20	-15	7.6	0.4	50	10

Moreover, in order to verifying the optimization result, the de-icing experiments of the composite material de-icing component were simplified and conducted. Thus, the temperature field numerical simulation of the rotor composite material de-icing component is effectively achieved. The experiment was conducted in a refrigeration box that the temperature is -15℃, the de-icing composite material component was fabricated by carbon fiber and glass fiber as shown in Fig. 1. The composite materials are pre-made materials that need co-curing under 80℃. The sample is shown in Fig.3.

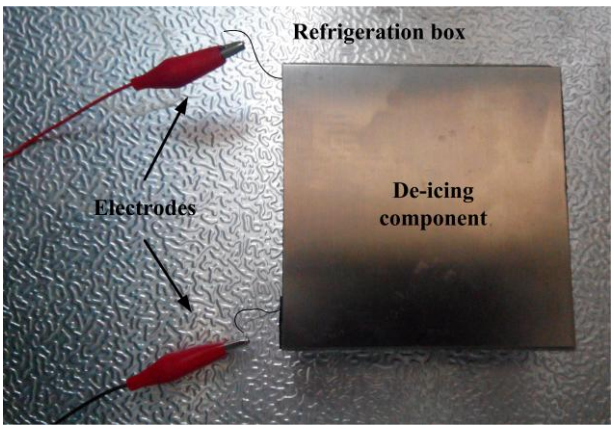

Fig.3. Schematic of composite material de-icing component sample.

The composite material de-icing component sample applied voltage: 15 V; current: 1.3 A; power: 19.5 W. The heated area is 100mm*100mm square stainless steel plate. The ice is formed on the de-icing component surface by spraying cold water from a 90mm*90mm mold to result in a frozen layer of 15mm thickness icing on the sample. The de-icing is set up before ice formation, and then the centrifugal force is employed by a tensionmeter. The schematic of de-icing experiment device is shown in Fig.4.

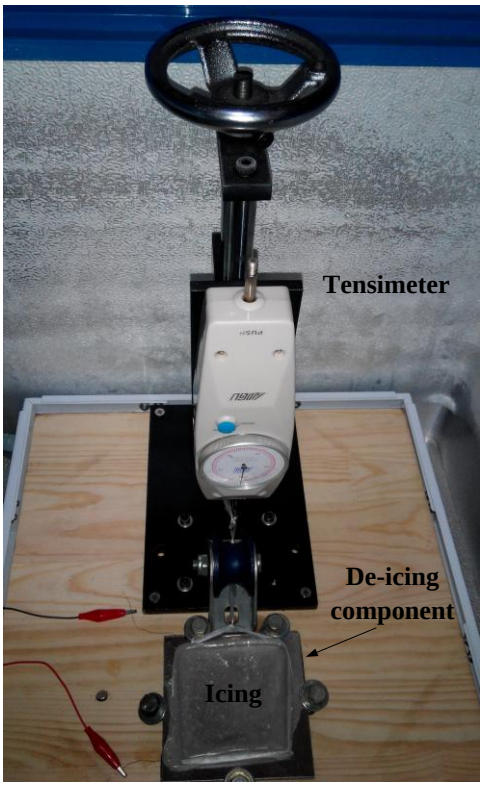

Fig.4. Schematic of de-icing experiment device.

The temperature on the surfaces in Test 17 (origin test) and Test 26 (optimized test) was measured. Fig.5 shows that the temperature distribution of the optimized test is faster to reach desired temperature than the origin one. By comparing the de-icing efficiency of origin and optimized tests, the optimized de-icing component shows outstanding performance in heat transfer and de-icing that can take shorter time in de-icing than origin test. Besides, the de-icing time of optimized test (98 seconds) is faster than the origin one (170 seconds), which increasing the efficiency of de-icing.

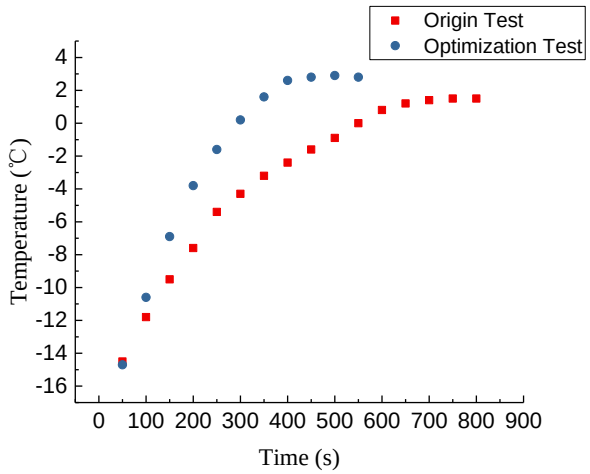

Fig.5. Comparison of temperature distribution.

Thus, experimental and simulation results show that the optimization effect is more evident than the non-optimized temperature distribution with the optimized results of the proposed method. Experimental results verify the effectiveness of the optimization method.

CONCLUSIONS

The numerical simulation model of the rotor composite material de-icing component is established based on numerical simulation method. The rotor composite material de-icing component temperature field distribution is optimized by employing orthogonal experiment. Based on the optimization, the following conclusions are presented:

(1) The factor that most significantly affects the uniform distribution of the temperature field on the rotor iron surface is electric voltage, followed by ambient temperature. Wind speed has the least influence.

(2) According to the minimum temperature difference on the rotor iron surface of rotor composite material de-icing component, the optimization parameters are selected as follows: the flow velocity is 20m/s, the layer heat transfer coefficient of thermal conductivity is 7.6W/(m·K), the ambient temperature is -15℃, the thickness of adhesive layer is 0.4mm, the power supply voltage is 50 V, and the distance of the heating wire is 10 mm.

ACKNOWLEDGEMENTS

This work was supported by the Defense Industrial Technology Development Program (No.A0520110009); the State Key Laboratory of Virtual Reality Technology Independent Subject (No.BUAA-VR-16ZZ-07); and the Beijing Municipal Natural Science Foundation (No.3172021). The authors thank the referees of this paper for their valuable and very helpful comments.

REFERENCES

[1] M. Pourbagian, W.G. Habashi, Aero-thermal optimization of in-flight electro-thermal ice protection systems in transient de-icing mode, *International Journal of Heat and Fluid Flow*, 54, 2015, pp. 167-182.

[2] H.J. Coffman, Helicopter rotor icing protection methods, *Journal of the American Helicopter Society*, 32(2), 1987, pp. 34-39.

[3] R.W. Gent, N.P. Dart, J.T. Cansdale, Aircraft icing. Philosophical Transactions of the Royal Society of London A: Mathematical, *Physical and Engineering Sciences*, 358(1776), 2000, pp. 2873-2911.

[4] W.H. Jang, D.K. Chan, S.J. Jae, A Study on the Parameters for Icing Airworthiness Flight Tests of Surion Military, *Helicopter*, 43(6), 2015, pp. 526-532.

[5] H.Y. Cao, G.Z. Li, R.A. Hess, Helicopter flight characteristics in icing conditions, *Aeronautical Journal*, 116(116), 2012, pp. 963-979.

[6] R. Elangovan, R.F. Olsen, Analysis of layered composite skin electro-thermal anti-icing system, *The 46th AIAA Aerospace Sciences Meeting and Exhibit*, 2008, pp. 1-15.

[7] H.J. Coffman, Review of helicopter icing protection systems, *American Institute of Aeronautics and Astronautics, Aircraft Design, Systems and Technology Meeting*, Fort Worth, TX, 17(19), 1983.

[8] G.W. Liu, B.F. Gao, G.H. Zhang, Study on helicopter icing intensity design standard, *Helicopter Technology*, 2011, pp. 30-33.

[9] X. Veillard, W.G. Habashi, M.S. Aube, Fensap-ice: Ice accretion in multi-stage jet engines, *The 47th AIAA Aerospace Sciences Meeting and Exhibit*, 4158, 2009.